In vivo determination of the optical properties of infant brain using frequency-domain near-infrared spectroscopy

Jun Zhao
Hai Shu Ding
Tsinghua University
Department of Biomedical Engineering
Beijing 100084, China
E-mail: dhs-dea@mail.tsinghua.edu.cn

Xin Lin Hou
Cong Le Zhou
First Hospital of Peking University
Department of Pediatrics
Beijing 100034, China

Britton Chance
University of Pennsylvania
Department of Biochemistry and Biophysics
Philadelphia, Pennsylvania 19104

Abstract. We investigate the optical properties of the brain in 23 neonates *in vivo* using a frequency domain near-infrared spectroscopy (NIRS). In this study, a calibration procedure is employed to determine the absorption and reduced scattering coefficients with single source-detector separation. The absorption coefficients of the infant foreheads are lower than the values reported in adults. A large intersubject variation in the reduced scattering coefficients is also demonstrated. Furthermore, physiological parameters are derived from the absorption coefficients at two wavelengths (788 and 832 nm). The mean total hemoglobin concentration (THC) is 39.7 ± 9.8 μM and the mean cerebral blood oxygen saturation (StO_2) is $58.7 \pm 11.2\%$. Our preliminary results show that this bedside frequent domain NIRS could provide quantitative optical measurement of the infant brain. [DOI: 10.1117/1.1891345]

Keywords: near-infrared spectroscopy; frequency domain; brain; infant.

Paper 04085 received Jun. 1, 2004; revised manuscript received Sep. 30, 2004; accepted for publication Oct. 11, 2004; published online; published online Apr. 4, 2005.

1 Introduction

The near-infrared (NIR) optical properties of tissue, namely absorption and reduced scattering coefficients, can provide information on a variety of tissue physiology processes. Wavelength-dependent absorption is widely used to quantify the concentration of biologically important chromophores, such as hemoglobin, water, and lipid. To date, scattering properties are not fully understood. Basically, the wavelength dependence of scattering is associated with tissue structure.

In the past decades, increasing use of light either as a diagnostic or therapeutic tool has demanded a better knowledge of the optical properties of human tissues.[1–4] The properties of the head, especially the neonatal brain, are not particularly well known. In recent years, great effort has been devoted to evaluating the optical properties of brain tissue.

Using integrating-sphere measurements, van der Zee, Essenpreis, and Delpy[5] determined the optical properties of postmortem neonate and adult human brain tissue over the wavelength range of 500 to 1000 nm. Yaroslavsky et al.[6] reported the optical properties of brain tissue *in vitro* from 360 to 1100 nm. However, due to significant alternation that may occur after the death of the organism, to obtain reliable information, it is important to estimate the optical properties *in vivo*.

The time-resolved method has proven to be a valuable tool to assess tissue optical properties *in vivo* noninvasively. Recently, *in vivo* optical properties of piglet brain[7] and adult forehead[8,9] were measured by time-resolved systems. Hebden et al.[10] obtained the first 3-D images of a premature infant brain using a 32-channel time-resolved imaging system. However, these measurements were obtained with a complex time-resolved system not suitable for clinical use. A frequency-domain apparatus, on the contrary, is relatively inexpensive and can easily be made portable, which are two important considerations for a clinically useful instrument.

Fantini et al.[11] and Hueber et al.[12] reported the optical properties of newborn piglet brain using a frequency-domain multidistance spectroscopy. Bevilacqua et al.[13] measured the local optical properties of normal and malignant human brain tissue *in vivo* during brain surgery with short source-detector separations. More recently, Choi et al.[14] published the measurements of absorption and reduced scattering coefficients through the forehead on 30 adult volunteers using a multidistance frequency-domain method. Up to now, however, published data on *in vivo* optical properties of neonatal brain in large populations, to the best of our knowledge, is relatively scarce.

Recently, we have developed a portable, multiwavelength, frequency-domain near-infrared spectroscopy (NIRS) instrument for quantitative, noninvasive measurement of tissue optical properties.[15,16] A calibration procedure was employed to quantify the absorption and reduced scattering coefficients with single source-detector separation. This instrument has been validated by extensive tissue equivalent phantom and animal experimental studies.[17,18] We investigated the optical properties of 23 infant heads using our frequency-domain NIRS instrument. The physiological parameters were also de-

Address all correspondence to Jun Zhao, (Department of) Biomedical Engineering, Tsinghua University, Haidian Distribution, Beijing 100084 China

1083-3668/2005/$22.00 © 2005 SPIE

rived from the absorption coefficients and compared with those available in the literature.

2 Theory and Method

2.1 *Algorithm*

The propagation of photons in tissue is well described by the radiation transport theory, and its simplification to the highly scattering regime results in the diffusion equation.[19–21] In frequency-domain systems, the light source is intensity modulated by a sinusoidal wave. The light energy propagates as a damped spherical wave outward from the source. This macroscopic scalar wave is often called the diffuse photon density wave (DPDW).[22–24] DPDW dispersion is highly dependent on the optical properties of the tissue.

Experimentally, we measured the reflectance, which is the number of photons crossing the tissue boundary per unit time per unit area at distance ρ. Pogue and Patterson[25] derived the expression for the ac component of reflectance $R(\rho,\omega,\mu_a,\mu_s',c_n)$ by application of the extrapolated boundary condition to the diffusion equation.

$$R(\rho,\omega,\mu_a,\mu_s',c_n)=\frac{1}{2(2\pi)^{3/2}}\left[\frac{z_0(1+k\rho_0)}{\rho_0^3}\exp(-k\rho_0)+\frac{z_p(1+k\rho_p)}{\rho_p^3}\exp(-k\rho_p)\right], \quad (1)$$

where

$$\rho_0^2=\rho^2+z_0^2,\quad \rho_p^2=\rho^2+z_p^2,\quad z_0=\frac{1}{\mu_s'},$$

$$z_p=z_0+\frac{4D}{s},\quad \kappa=\left(\frac{\mu_a c_n+i\omega}{Dc_n}\right)^{1/2},\quad D=\frac{1}{3(\mu_a+\mu_s')},$$

and s is a constant that depends on the refractive index mismatch ($s=0.4258$ for a tissue-air boundary).

Note that the measured reflectance $R(\rho,\omega,\mu_a,\mu_s',c_n)$ is complex. The phase of the ac component of the reflectance is given by

$$\theta=\tan^{-1}\frac{\mathrm{Im}[R]}{\mathrm{Re}[R]}, \quad (2)$$

and the amplitude is

$$A=(\mathrm{Re}^2[R]+\mathrm{Im}^2[R])^{1/2}. \quad (3)$$

The measured amplitude and phase on the infant heads were first normalized by the amplitude and phase measured on a reference phantom, then fitted in Eq. (1) (Levenberg-Marquardt nonlinear fitting) to estimate the absorption coefficient μ_a and reduced scattering coefficient μ_s'.

2.2 *Derivation of Physiological Parameters*

We assume that the chromophores contributing to μ_a in the brain tissue are principally oxy- and deoxyhemoglobin:

$$\mu_a^\lambda=\epsilon_{\mathrm{Hb}}^\lambda[\mathrm{Hb}]+\epsilon_{\mathrm{HbO_2}}^\lambda[\mathrm{HbO_2}], \quad (4)$$

where μ_a^λ is the absorption coefficient at wavelength λ, $\epsilon_{\mathrm{chrom}}^\lambda$ is the extinction coefficient of a given chromophore at wavelength λ, and [Hb] and [HbO_2] are the concentration of hemoglobin and oxygenated hemoglobin, respectively.

In this study, the absorption coefficients obtained at two wavelengths (i.e., 788 and 832 nm) were employed to calculate the [Hb] and [HbO_2]. $\epsilon_{\mathrm{Hb}}^\lambda$ and $\epsilon_{\mathrm{HbO_2}}^\lambda$ were obtained from the literature.[26,27]

Two physiologically important parameters, namely tissue oxygen saturation (StO_2) and total hemoglobin concentration (THC), could be derived from [Hb] and [HbO_2].

$$\mathrm{StO_2}(\%)=\frac{[\mathrm{HbO_2}]}{[\mathrm{Hb}]+[\mathrm{HbO_2}]}\times 100, \quad (5)$$

$$\mathrm{THC}=[\mathrm{Hb}]+[\mathrm{HbO_2}]. \quad (6)$$

3 Instrumentation and Calibration

3.1 *Frequency-Domain NIRS Instrument*

This study has been performed with a homodyne frequency-domain NIRS instrument (see Fig. 1), which was described in detail elsewhere.[15,16] Briefly, this frequency-domain NIRS instrument uses three laser diodes at 788-, 814-, and 832-nm wavelength. The three wavelengths are time multiplexed at a rate of 1 Hz. The light is modulated at 140 MHz and directed to the forehead of neonates by a 1-mm-diam fiber guide. The diffused light is collected to the photomultiplier tube (PMT, Hamamatsu, H7683-02) by another 3-mm-diam fiber bundle, placed several centimeters apart from the source fiber. The amplitude and phase shift of the detected photon density wave can be further derived from the output of the in-phase and quadrature demodulator (Mini-Circuit, MIQY-140D).

$$\theta=\tan^{-1}\frac{Q_{dc}}{I_{dc}}, \quad (7)$$

$$A=(I_{dc}^2+Q_{dc}^2)^{1/2}. \quad (8)$$

3.2 *Instrument Calibration*

It is noted that the measured phase and amplitude of photon density waves include contribution from both the sample and the instrument.[16,28] The measured phase is the sum of the sample and instrument phase, while the measured amplitude is the product of the sample and instrument amplitude. Two kinds of calibration procedure can be used to remove the instrument response from the raw data: the multidistance method and use of a standard reference phantom calibration. The first approach works well in a macroscopically homogeneous turbid medium, while the latter is more effective for heterogeneous *in vivo* measurements.[28]

In this study, a standard reference phantom with known optical properties was employed to remove the instrument response from the raw data. The phantom was made of a pliable RTV silicon resin. A calculated amount of TiO_2 powder and carbon black powder were added to the resin to obtain the expected reduced scattering coefficient and absorption coefficient, respectively. The optical properties of the calibration phantom had been previously determined by measurements

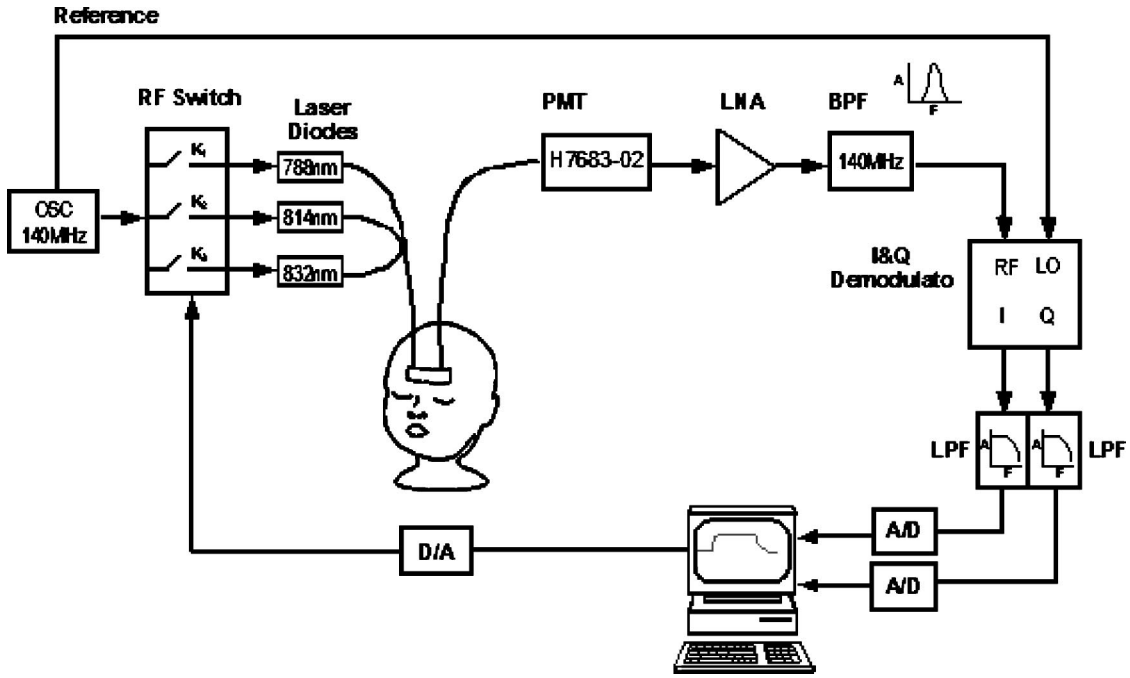

Fig. 1 Schematic diagram of the frequency-domain NIRS instrument. OSC is the oscillator; PMT is the photomultiplier tube; LNA is the low noise amplifier; BPF is the bandpass filter; I and Q are the in phase and quadrature phase; LPF is the low pass filter; D/A is the digital-to-analog converter; and A/D is the analog-to-digital converter.

using the multidistance method.[23,29] To match the shape of the infant heads, the calibration phantom was cylindrically molded with a radius of curvature of 5.5 cm.

4 Experimental Protocol

23 infants were enrolled in this study. They had a median gestional age of 39 (range 35 to 42.5) weeks, a body weight of 3200 (2400 to 4600) g, and a postnatal age of 5 (1 to 17) days. Two of them were preterm infants with a gestional age of 35 and 36 weeks, respectively. The subjects were admitted due some diseases but were all in recovery at the time of study and had normal cranial ultrasound scans: mild jaundice ($n=12$), pneumonia ($n=3$), hypoglycemia ($n=2$), and healthy infants ($n=6$). Informed parental consent was obtained before each investigation.

The subjects were in a supine, comfortable position during the entire experiment. Measurements were performed on each subject by gently placing the probe on the forehead. Just enough pressure was applied to ensure optical contact between skin and probe. At least two measurements were performed successively at a given location to exclude the problem of optical coupling. Sometimes we changed the position a little bit for better contact.

The source-detector separation of the probe was fixed at 4 cm, which means the frequency-domain NIRS instrument views a banana-shaped tissue volume between the emitter and detector located approximately 1 to 3 cm beneath the skin.[3,9] With the probe on the forehead, this instrument appears to monitor both gray and white matter in the frontal neocortex.

The calibration procedures were performed right before or after the measurements. The top and bottom sides of the cylindrical silicon resin phantom were covered with aluminum foil to simulate the semi-infinite boundary condition.

5 Results and Discussion

5.1 *Optical Properties*

Figure 2 shows the histograms of the fitted absorption coefficient μ_a and reduced scattering coefficient μ_s' in 23 infant foreheads at wavelengths of 788 and 832 nm, respectively. The vertical axis in each histogram is the number of subjects. Mean and standard deviation of the fitted optical properties are listed in Table 1.

Note that the absorption coefficients of the infant foreheads are lower than the values reported in adults.[8,9,14] This difference may partly be due to the brain itself, and partly due to the influence of the superficial layer. NIRS monitors the tissue beneath the optical fiber, which includes scalp (skin, subcutaneous fat, muscle), skull, cerebrospinal fluid (CSF), and the brain. The measurement of an adult head may be contaminated by these layered structures. In infants, however, the thin extracerebral tissues (<5 mm) do not significantly contaminate the measurement of optical properties from the surface of the head.[30]

The broadly distributed μ_s' in Fig. 2 may be due to the large intersubject variation. In other words, the variation of μ_s' should be taken into account when comparing data among subjects. However, the current commercially available continuous-wave NIRS cannot separate the effect of scattering from the attenuation of light and thus simply assumes a constant μ_s'. Frequency-domain NIRS allows separation of μ_a and μ_s', which make it possible to provide absolute concentration of Hb and HbO_2.

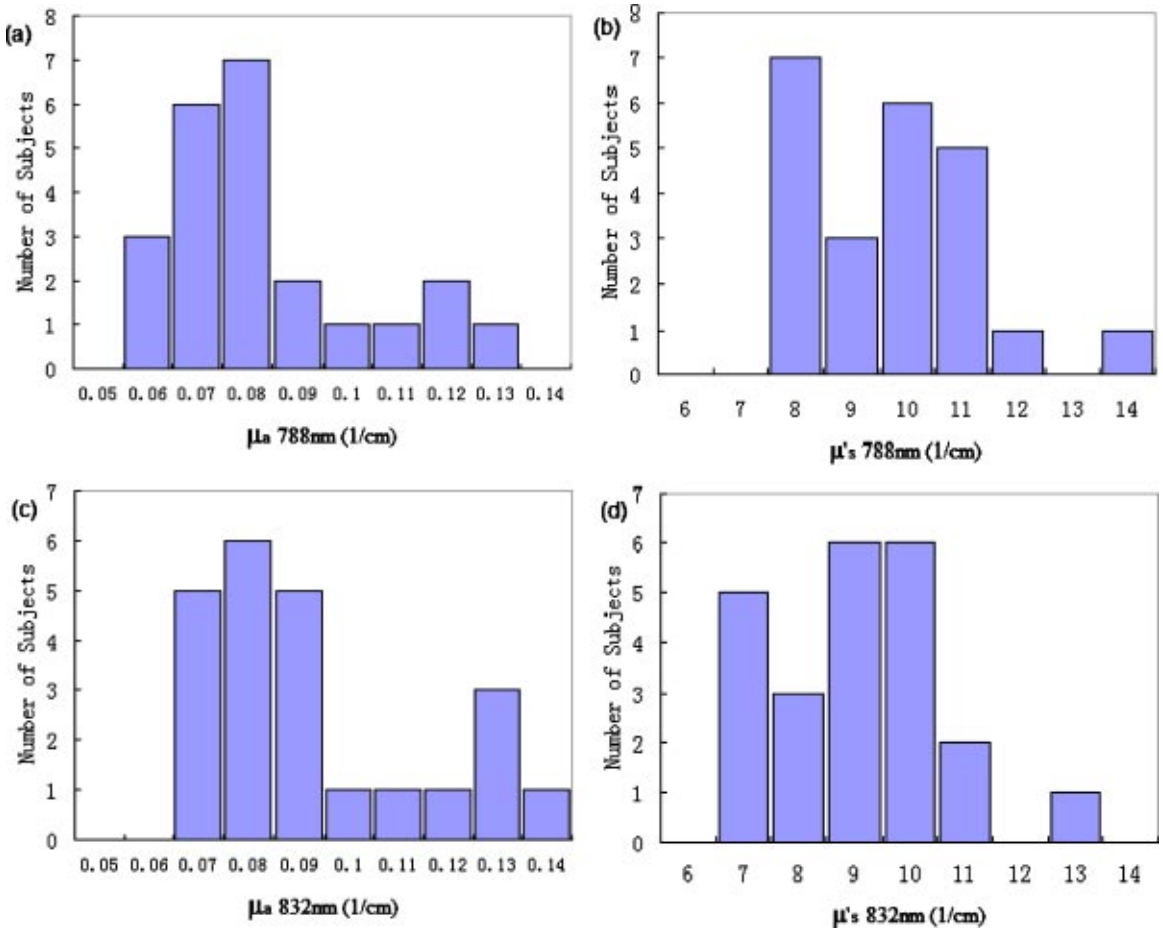

Fig. 2 Histograms of the fitted μ_a and μ_s' in 23 infant foreheads at wavelengths of 788 and 832 nm, respectively. The vertical axis in each histogram is the number of subjects. The source-detector separation is 4 cm.

5.2 *Physiological Parameters*

Histograms of the physiological properties extracted from μ_a values are summarized in Fig. 3. Note that we have ignored the background absorption and used absorption coefficients at two wavelengths to derive the hemoglobin concentration. Despite the simplistic assumptions involved, the physiological properties derived from the absorption coefficients (Table 1) agree reasonably well with the results available in the literature.

Table 1 Average optical properties, physiological parameters, and standard deviation of brain in 23 infants.

λ (nm)	788	832
μ_a (cm^{-1})	0.078±0.014	0.089±0.019
μ_s' (cm^{-1})	9.16±1.22	8.42±1.23
[Hb] (μM)	16.0±5.1	
[HbO_2] (μM)	23.7±8.4	
THC (μM)	39.7±9.8	
StO_2(%)	58.7±11.2	

Cooper et al.[31] measured 19 newborn infants with second differential spectroscopy. Their preliminary results gave a mean deoxyhemoglobin concentration of 14.6±4.0 μM, which is consistent with our result (16.0±5.1 μM). NIRS measurements of absolute cerebral hemoglobin concentrations in neonates by Wolf et al.[32] found an average tissue oxygen saturation (StO_2) of about 66±4%, while we obtain a somewhat lower value of 58.7±11.2%. Wyatt et al.[33] reported the mean cerebral blood volume of the infant brain (2.2±0.4 ml per 100 g of tissue). This corresponds to an estimated total hemoglobin concentration (THC) of 36±11 μM of tissue, which agrees well with our average of 39.7±9.8 μM.

5.3 *Reproducibility of the Optical Measurements*

The reproducibility of our optical measurements were assessed by successive reposition of the optical probe on the same spot. 15 infants were measured just after they were fed. They were all quiet during the measurements. In fact, most of them were asleep. Since optical coupling is one of the main sources of reproducibility errors, all measurements were per-

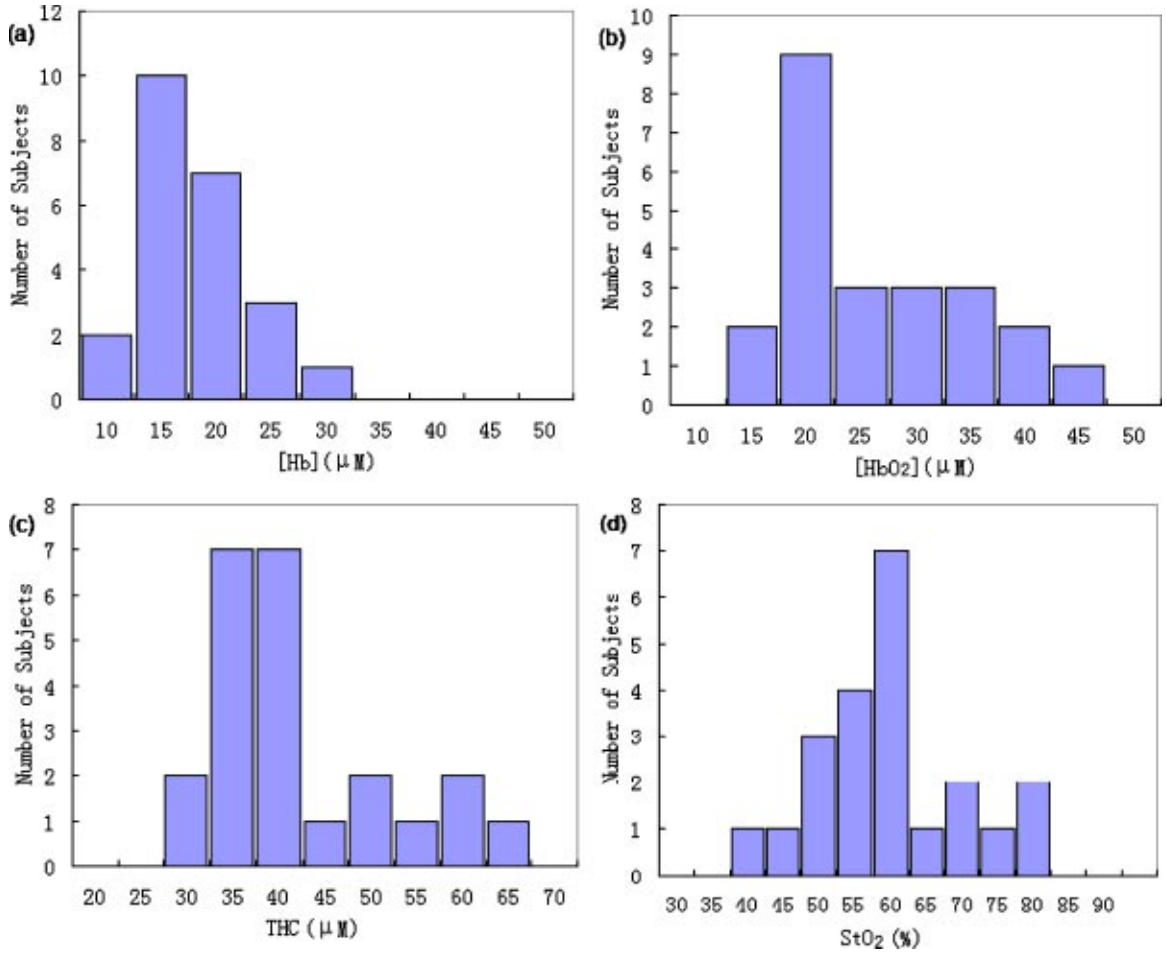

Fig. 3 Histograms of [Hb], [HbO_2], total hemoglobin concentration (THC), and tissue oxygen saturation (StO_2) derived from absorption coefficients. The vertical axis in each histogram is the number of subjects. The source-detector separation is 4 cm.

formed by the same experimenter using a consistent pressure. Five measurements were performed consecutively per infant. Reproducibility is based on the maximum difference in the parameters as a result of repeated repositioning of the optical probe on the same spot.[11] The reproducibility errors estimate the uncertainty in the absolute readings. The average results of 15 infants are listed in Table 2. It suggests that the results were repeatable in quiet situations. However, an optical probe that could tolerate extensive movements is still desirable, especially in the study of the infants.

6 Discussion

The main clinical interest in NIRS was initially for monitoring brain oxygenation in newborn babies. NIRS has been used for perinatal application since 1985, and hundreds of studies have been performed.[34,35] Used in a research context, NIRS has improved understanding of cerebral circulation. However, NIRS is used infrequently to guide clinical care because of quantitation problems related to the biophysics of measurement.

The improved NIRS technologies, such as time- and frequency-resolved NIRS enables experimenters to separate tissue scattering effects from tissue absorption effects, and thus extract more quantitative information about tissue chromophores. In this work, a novel frequency-domain method was employed to quantify the optical properties of infant brains. However, several points should be considered during the interpretation of the experimental data.

First, the measurements were obtained with a single source-detector separation (4 cm). The NIRS instrument

Table 2 Average reproducibility errors of optical measurements in 15 infants. Reproducibility of absolute measurements is based on the maximum difference in the parameters as a result of successive reposition of the probe on the same spot.

λ (nm)	788	832
$\Delta\mu_a$ (cm^{-1})	0.0027	0.0034
$\Delta\mu_s'$ (cm^{-1})	0.30	0.31
Δ[Hb] (μM)	0.77	
Δ[HbO_2] (μM)	1.17	
ΔTHC (μM)	1.54	
ΔStO_2(%)	1.63	

views a banana-shaped tissue volume including the scalp, skull, cerebrospinal fluid (CSF), and the brain. In newborn infants, the thin extracerebral tissues make it possible to detect more information from both gray and white matter in the frontal neocortex.[30] In adults, however, the interference from the thicker extracranial tissues cannot be ignored.[36] To obtain depth information on different layers, the multiple-distance method could be introduced in adult brain applications.[14,37]

Secondly, a simplified model of light propagation (homogeneity and semi-infinite boundary condition) was employed to recover the optical properties of tissue from the experimental data. The neonatal head, however, was both highly inhomogeneous and curved. The difference between the actual anatomy and model may induce systematic errors. Analytical solutions of the diffusion equation for more accurate sphere and cylinder geometries are also available in the literature.[25,38] Unfortunately, they are time consuming and not suitable for real-time application.

Finally, we assumed that oxy- and deoxyhemoglobin are the primary chromophores in the brain when deriving the physiological properties from μ_a at two wavelengths (788 and 832 nm). In brain tissue, hemoglobin, water, and cytochrome-c oxidase are known chromophores in the near-infrared region.[27] The accuracy of quantitative hemoglobin concentration may be hindered by ignoring the nonhemoglobin absorption.

There are also some practical limitations to obtaining the quantitative measurements of infant brains, which have not been discussed here. The main concern of this work is to investigate the potential of this novel frequency-domain NIRS in pediatric applications. The baseline of the optical and physiological properties of infant brains was obtained. Work is in progress to improve the instrument and to design more complex measurement protocols for assessment of infant brain injury and neurodevelopment.

7 Conclusions

We present determination of *in vivo* optical properties of 23 neonatal foreheads using a portable frequency-domain NIRS instrument. A calibration phantom of known optical properties is employed to quantify the absorption coefficient and reduced scattering coefficient with a single source-detector separation. The ability to separate tissue scattering effects from tissue absorption effects makes it possible to obtain quantitative measurements. Physiological parameters derived from the measured absorption coefficients are consistent with those in the literature. The factors affecting the interpretation of the experimental data are also discussed, which suggests considerable work remains to assess the utility of this approach in clinical practice.

References

1. A. Villringer and B. Chance, ''Non-invasive optical spectroscopy and imaging of human brain function,'' *Trends Neurosci.* **20**(10), 435–442 (1997).
2. T. H. Pham, O. Coquoz, J. B. Fishkin, E. Anderson, and B. J. Tromberg, ''Broad bandwidth frequency domain instrument for quantitative tissue optical spectroscopy,'' *Rev. Sci. Instrum.* **71**(6), 2500–2513 (2000).
3. E. Gratton, S. Fantini, M. A. Franceschini, G. Gratton, and M. Fabiani, ''Measurement of scattering and absorption changes in muscle and brain,'' *Philos. Trans. R. Soc. London, Ser. B* **352**, 727–735 (1997).
4. M. Wolf, U. Wolf, J. H. Choi, V. Toronov, L. A. Paunescu, A. Michalos, and E. Gratton, ''Fast cerebral functional signal in the 100-ms range detected in the visual cortex by frequency-domain near-infrared spectrophotometry,'' *Psychophysiology* **40**(4), 521–528 (2003).
5. P. van der Zee, M. Essenpreis, and D. T. Delpy, ''Optical properties of brain tissue,'' *Proc. SPIE* **1888**, 454–465 (1993).
6. A. N. Yaroslavsky, P. C. Schulze, I. V. Yaroslavsky, R. Schober, F. Ulrich, and H. J. Schwarzmaier, ''Optical properties of selected native and coagulated human brain tissues *in vitro* in the visible and near infrared spectral range,'' *Phys. Med. Biol.* **47**, 2059–2073 (2002).
7. A. Sassaroli, F. Martelli, Y. Tanikawa, K. Tanaka, R. Araki, Y. Onodera, and Y. Yamada, ''Time-resolved measurements of *in vivo* optical properties of piglet brain,'' *Opt. Rev.* **7**(5), 420–425 (2000).
8. S. J. Matcher, M. Cope, and D. T. Delpy, ''*In vivo* measurements of the wavelength dependence of tissue-scattering coefficients between 760 and 900 nm measured with time-resolved spectroscopy,'' *Appl. Opt.* **36**(1), 386–396 (1997).
9. A. Torricelli, A. Pifferi, P. Taroni, E. Giambattistelli, and R. Cubeddu, ''*In vivo* optical characterization of human tissues from 610 to 1010 nm by time-resolved reflectance spectroscopy,'' *Phys. Med. Biol.* **46**, 2227–2237 (2001).
10. J. C. Hebden, A. Gibson, R. M. Yusof, N. Everdell, E. M. C. Hillman, D. T. Delpy, S. R. Arridge, T. Austin, J. H. Meek, and J. S. Wyatt, ''Three-dimensional optical tomography of the premature infant brain,'' *Phys. Med. Biol.* **47**, 4155–4166 (2002).
11. S. Fantini, D. Hueber, M. A. Franceschini, E. Gratton, W. Rosenfeld, P. G. Stubblefield, D. Maulk, and M. R. Stankovic, ''Non-invasive optical monitoring of the newborn piglet brain using continous-wave and frequency-domain spectroscopy,'' *Phys. Med. Biol.* **44**, 1543–1563 (1999).
12. D. M. Hueber, M. A. Franceschini, H. Y. Ma, Q. Zhang, J. R. Ballesteros, S. Fantini, D. Wallace, V. Ntziachristos, and B. Chance, ''Non-invasive and quantitative near-infrared haemoglobin spectrometry in the piglet brain during hypoxic stress, using a frequency-domain multidistance instrument,'' *Phys. Med. Biol.* **46**, 41–62 (2001).
13. F. Bevilacqua, D. Piguet, P. Marquet, J. D. Gross, B. J. Tromberg, and C. Depeursinge, ''*In vivo* local determination of tissue optical properties: applications to human brain,'' *Appl. Opt.* **38**(22), 4939–4950 (1999).
14. J. Choi, M. Wolf, V. Toronov, U. Wolf, C. Polzonetti, D. Hueber, L. P. Safonova, R. Gupta, A. Michalos, W. Mantulin, and E. Gratton, ''Noninvasive determination of the optical properties of adult brain: near-infrared spectroscopy approach,'' *J. Biomed. Opt.* **9**(1), 221–229 (2004).
15. Y. S. Yang, H. L. Liu, X. D. Li, and B. Chance, ''Low-cost frequency-domain photon migration instrument for tissue spectroscopy, oximetry, and imaging,'' *Opt. Eng.* **36**(5), 1562–1569 (1997).
16. B. Chance, M. Cope, E. Gratton, N. Ramanujam, and B. Tromberg, ''Phase measurement of light absorption and scatter in human tissue,'' *Rev. Sci. Instrum.* **69**(10), 3457–3481 (1998).
17. H. Y. Ma, Q. Xu, J. R. Ballesteros, V. Ntziachristos, Q. Zhang, and B. Chance, ''Quantitative study of hypoxia stress in piglet brain by IQ phase modulation oximeter,'' *Proc. SPIE* **3597**, 642–649 (1999).
18. Y. Chen, R. T. Dharmesh, X. Intes, and B. Chance, ''Correlation between near-infrared spectroscopy and magnetic resonance imaging of rat brain oxygenation modulation,'' *Phys. Med. Biol.* **48**(4), 417–427 (2003).
19. M. S. Patterson, B. Chance, and B. C. Wilson, ''Time resolved reflectance and transmittance for the non-invasive measurement of tissue optical properties,'' *Appl. Opt.* **26**(12), 2331–2336 (1989).
20. M. S. Patterson, J. D. Moulton, B. C. Wilson, K. W. Berndt, and J. R. Lakowicz, ''Frequency-domain reflectance for the determination of the scattering and absorption properties of tissue,'' *Appl. Opt.* **30**(31), 4474–4476 (1991).
21. R. C. Haskell, L. O. Svaasand, T. T. Tsay, T. C. Feng, M. S. McAdams, and B. J. Tromberg, ''Boundary conditions for the diffusion equation in radiative transfer,'' *J. Opt. Soc. Am. A* **11**(10), 2727–2741 (1994).
22. M. A. O'Leary, D. A. Boas, B. Chance, and A. G. Yodh, ''Refraction of diffuse photon density waves,'' *Phys. Rev. Lett.* **69**, 2658 (1992).
23. J. B. Fishkin and E. Gratton, ''Propagation of photon-density waves in strongly scattering media containing an absorbing semi-infinite

plane bounded by a straight edge,'' *J. Opt. Soc. Am. A* **10**(1), 127–140 (1993).
24. B. J. Tromberg, L. O. Svaasand, T. T. Tsay, and R. C. Haskell, ''Properties of photon density waves in multiple-scattering media,'' *Appl. Opt.* **32**, 607–616 (1993).
25. B. W. Pogue and M. S. Patterson, ''Frequency-domain optical-absorption spectroscopy of finite tissue volumes using diffusion-theory,'' *Phys. Med. Biol.* **39**, 1157–1180 (1994).
26. M. Cope, PhD Thesis, Dept. of Medical Physics and Bioengineering, Univ. College London (1991).
27. S. J. Matcher, C. E. Elwell, C. E. Cooper, M. Cope, and D. T. Delpy, ''Performance comparison of several published tissue near-infrared sepctroscopy algorithms,'' *Anal. Biochem.* **227**, 54–68 (1995).
28. B. J. Tromberg, O. Coquoz, J. B. Fishkin, T. Pham, E. Anderson, J. Butler, M. Cahn, J. D. Gross, V. Venugopalan, and D. Pham, ''Non-invasive measurements of breast tissue optical properties using frequency-domain photon migration,'' *Philos. Trans. R. Soc. London, Ser. B* **352**, 661–668 (1997).
29. S. Fantini, M. A. Franceschini, and E. Gratton, ''Semi-infinite-geometry boundary problem for light migration in highly scattering media: a frequency-domain study in the diffusion approximation,'' *J. Opt. Soc. Am. B* **11**(10), 2128–2138 (1994).
30. C. D. Kurth and W. S. Thayer, ''A multiwavelength frequency-domain near-infrared cerebral oximeter,'' *Phys. Med. Biol.* **44**, 727–740 (1999).
31. C. E. Cooper, C. E. ElWell, J. H. Meek, S. J. Matcher, J. S. Wyatt, M. Cope, and D. T. Delpy, ''The noninvasive measurement of absolute cerebral deoxyhemoglobin concentration and mean optical path length in the neonatal brain by second derivative near infrared spectroscopy,'' *Pediatr. Res.* **39**(1), 32–38 (1996).
32. M. Wolf, P. Evans, H. U. Bucher, V. Dietz, M. Keel, R. Strebel, and K. von Siebenthal, ''The measurement of absolute cerebral hemoglobin concentration in adults and neonates,'' *Adv. Exp. Med. Biol.* **428**, 219–227 (1997).
33. J. S. Wyatt, M. Cope, D. T. Delpy, C. E. Richardson, A. D. Edwards, S. Wray, and E. O. R. Reynolds, ''Quantitation of cerebral blood volume in human infants by near-infrared spectroscopy,'' *J. Appl. Phys.* **68**(3), 1086–1091 (1990).
34. J. E. Brazy, V. Darrell, M. D. Lewis, M. H. Mitnick, and F. F. Jobsis, ''Nonivasive monitoring of cerebral oxygenation in preterm infants: preliminary observations,'' *Pediatrics* **75**, 217–225 (1985).
35. S. E. Nicklin, I. A. A. Hassan, Y. A. Wickramasinghe, and S. A. Spencer, ''The light still shines, but not that brightly? The current status of perinatal near infrared spectroscopy,'' *Arch. Dis. Child* **88**(4), 263–268 (2003).
36. E. Okada, M. Firbank, M. Schweiger, S. R. Arridge, M. Cope, and D. T. Delpy, ''Theoretical and experimental investigation of near-infrared light propagation in a model of the adult head,'' *Appl. Opt.* **36**(1), 21–31 (1997).
37. M. A. Franceschini, S. Fantini, L. A. Paunescu, J. S. Maier, and E. Gratton, ''Influence of a superficial layer in the quantitative spectroscopic study of strongly scattering media,'' *Appl. Opt.* **37**(31), 7447–7458 (1998).
38. S. R. Arridge, M. Cope, and D. T. Delpy, ''The theoretical basis for the determination of optical pathlengths in tissue: temporal and frequency analysis,'' *Phys. Med. Biol.* **37**, 1531–1560 (1992).